Supplementary Materials for

Functional diversity of human intrinsically photosensitive retinal ganglion cells

Ludovic S. Mure*, Frans Vinberg, Anne Hanneken, Satchidananda Panda*

*Corresponding author. Email: lmure@salk.edu (L.S.M.); panda@salk.edu (S.P.)

Published 6 December 2019, *Science* **366**, 1251 (2019)
DOI: 10.1126/science.aaz0898

This PDF file includes:

Materials and Methods

Donors: Post-mortem human eyes were obtained through the San Diego Eye Bank and Lifesharing with ethical approval from the Scripps Health Investigational Review Board. Whole eye globes were enucleated and placed into oxygenated Ames' under bright surgical light within 1/2-5 hours (details about the eyes are summarized in **TableS1)**. They were immediately transported to the site of electrophysiology experiments at the Salk Institute in a light-tight container and all the subsequent procedures were conducted under dim red light. Cornea, lens and most of the vitreous were removed immediately after transportation and the posterior eyecups were kept in darkness for an additional hour to allow pigment regeneration via retinal pigment epithelium. For each donors, both eyes were used. Patches of the retina (4 or 6 mm in diameter) centered at ~3 mm from the optic nerve were punched through vitreous and pieces of the neural retina were stored in continuously oxygenated Ames' medium in darkness until the start of the electrophysiology experiments (2-7 hours after death).

Mice: All animal care and procedures were approved by the Institutional Animal Care and Use Committee of the Salk Institute for Biological Studies. C3H/HeJ strain (*rd*) carrying *Pde6b*^{rd1} mutation was obtained from the Jackson Laboratory. These mice are deficient in the β-subunit of phosphodiesterase that results in rapid rods death followed by cones loss. Mice were housed under 12-hr light:12-hr dark cycles (lights on at 6 AM). Standard laboratory chow and water were available *ad libitum*. All recordings were performed on retina obtained from 8-10 weeks old animals between 9 AM to 12 PM.

Multi Electrodes Array (MEA) recording: Patches of retina were mounted on MEA (Multichannel Systems, Reutlingen, Germany), ganglion cell side down, and perfused with oxygenated Ames' medium (Sigma-Aldrich, A1420-10X1L) at 34°C supplemented with 20 μM CNQX and 50 μM D-APV to block glutamatergic transmission. The activity of ganglion cells was recorded via 256 electrodes 30 μm in diameter spaced every 100 μm apart and arranged in a 16 × 16 square grid. Full-field visual stimuli at flux from ~$5x10^{11}$ to $5x10^{14}$ photons/cm^2/s at the retina were presented during recordings using high brightness LED (LuxeonStar 5, luxeonstar.com) at wavelengths of 447, 470, 505, 530, and 560 nm. The current through the LEDs was controlled using custom electronics and software written in MATLAB (Mathworks, Natick, MA) and synchronized with the physiological recording with a resolution of ± 100 μs. The signal was acquired from all 256 channels @ 10 kHz. Negative thresholds for spike detection were set at 5 times the standard deviation of the noise on each channel. Spike cutouts, consisting of 1 msec preceding and 2 msec after a suprathreshold event, along with a timestamp of the trigger was written to hard disk. For each electrode, these spike cutouts were sorted into trains of a single cell after recording using Offline Sorter (Plexon, Denton, TX). Data analysis and display were performed using Neuroexplorer (Plexon) and custom software written in MATLAB. Opsinamide (AA92593) was obtained through Princeton BioMolecular Research (NJ, US) and supplemented to Ames' medium at 10 μM in dissolved in DMSO (0.1%).

11-cis retinaldehyde was obtained through NEI (https://www.nei.nih.gov/funding/11_cis_retinal). For the chromophore supply experiment, the regular recording medium was switched to the same Ames' medium supplemented with ~25 μM *11-cis* retinal dissolved in 0.1% ethanol, a concentration in the range of retinoids use in mouse studies (*17*, *23*) and the estimation for the human eye (*24*, *25*).

Analysis: The response discharge rate was calculated as the average of the discharge rate measured during the stimulation (30s unless otherwise stated) minus the average discharge rate measure during the 30s prior to the stimulation (baseline). The response latency was defined as the delay between the start of the stimulation and the response crossing a threshold set at baseline +2*SD. The response was considered over after firing rate dropped below the baseline level for more than 3 seconds. The dose-response curve (DRC) was obtained by plotting the response (Y, discharge rate) as a function of the irradiance of the stimulation (X, photon/cm^2/s). For types 1 and 2, the DRC was fitted by a Michaelis-Menten function of the form; Y=Rmax*X/(EC50+X) where Rmax is the maximum response (discharge rate) and EC50 is the irradiance required to drive a 50 percent response. Relative sensitivity for each wavelength was estimated by multiplying the inverse of the EC50 at this wavelength by the EC50 for the wavelength of greatest sensitivity (lowest EC50). The average relative sensitivity was plotted against Lamb templates of Vitamin A based pigment spectral sensitivity of varying wavelengths (*19*), and the sum of least squares was calculated to find the curve with the best fit to our measured data. The peak of this curve was assigned as the λmax of human ipRGCs. Custom Matlab codes were used for all analyses. Given the limited range of responses displayed by type 3 cells, we did not fit their DRC by a Michaelis-Menten function but simply performed a linear regression to approximate half-saturation values.

ipRGCs clustering: Responses of adult ipRGCs to 470 nm light at four different intensities (2.9x10^{11}, 3.5 x10^{12}, 2 x10^{13}, and 2x10^{14} photons/cm^2/s) were utilized using light-induced spike trains parameters. As in each donor, time course, sensitivity, and duration of the ipRGCs

responses were visually segregated in two populations, we performed k-means clustering on these different parameters. Time course and duration were normalized to the maximum to allow for comparison between donors. Independently from the initial value of clusters we input, ipRGCs response time course, sensitivity, and duration always formed two main groups. Hierarchical clustering leads to the same results.

As for extracellular MEA recordings, Tu et al. (2005) (*3*) used latency in addition to sensitivity to distinguish functional types of ipRGCs in the mouse, we performed principal component analysis (PCA) on sensitivity, duration, and latency of the response. PCA allowed reducing the dimensionality of the data set; the first two principal components accounted for almost 95% of the variance (PC1=79.1% and PC2=14.6%). Thus, we next performed k-means clustering analysis on the first two principal components. This model produced clusters that corresponded to the initial analysis.

To objectively determine the number of clusters, ipRGCs first two principal components were fit with Gaussian mixture distributions or Gaussian mixture models (GMMs). We produced separate GMMs for 1, 2, and 3 ipRGCs clusters and then used the Akaike information criterion (AIC) to determine which GMM reported best the ipRGCs distribution. AIC is a model selection tool used to compare multiple models fit the same data. AIC is a likelihood-based measure of model fit that includes a penalty for complexity, specifically, the number of parameters. When we compared the 1, 2, and 3 cluster models, the model with the smallest AIC value (best model) was the 2 clusters model.

Results obtained in presence of 11-cis retinal were analyzed similarly. When pulled and analyzed all together recordings performed with and without exogenous 11-cis retinal, GMM models (1 to 4 clusters) and AIC comparison now pointed out the 3 clusters model as best fitting the data.

Matlab (2019a) was used for k-means and hierarchical clusterings, PCA, GMM, and AIC analysis (Statistics and Machine Learning Toolbox).

Quantification and Statistical Analysis

All data are expressed as means ± SEM or median and whiskers box (10th to 90th percentiles) unless stated otherwise. GraphPad Prism was used for all statistical analyses. Statistical tests used are stated in the figures legends. Differences between groups were considered statistically significant for $p<0.05$.

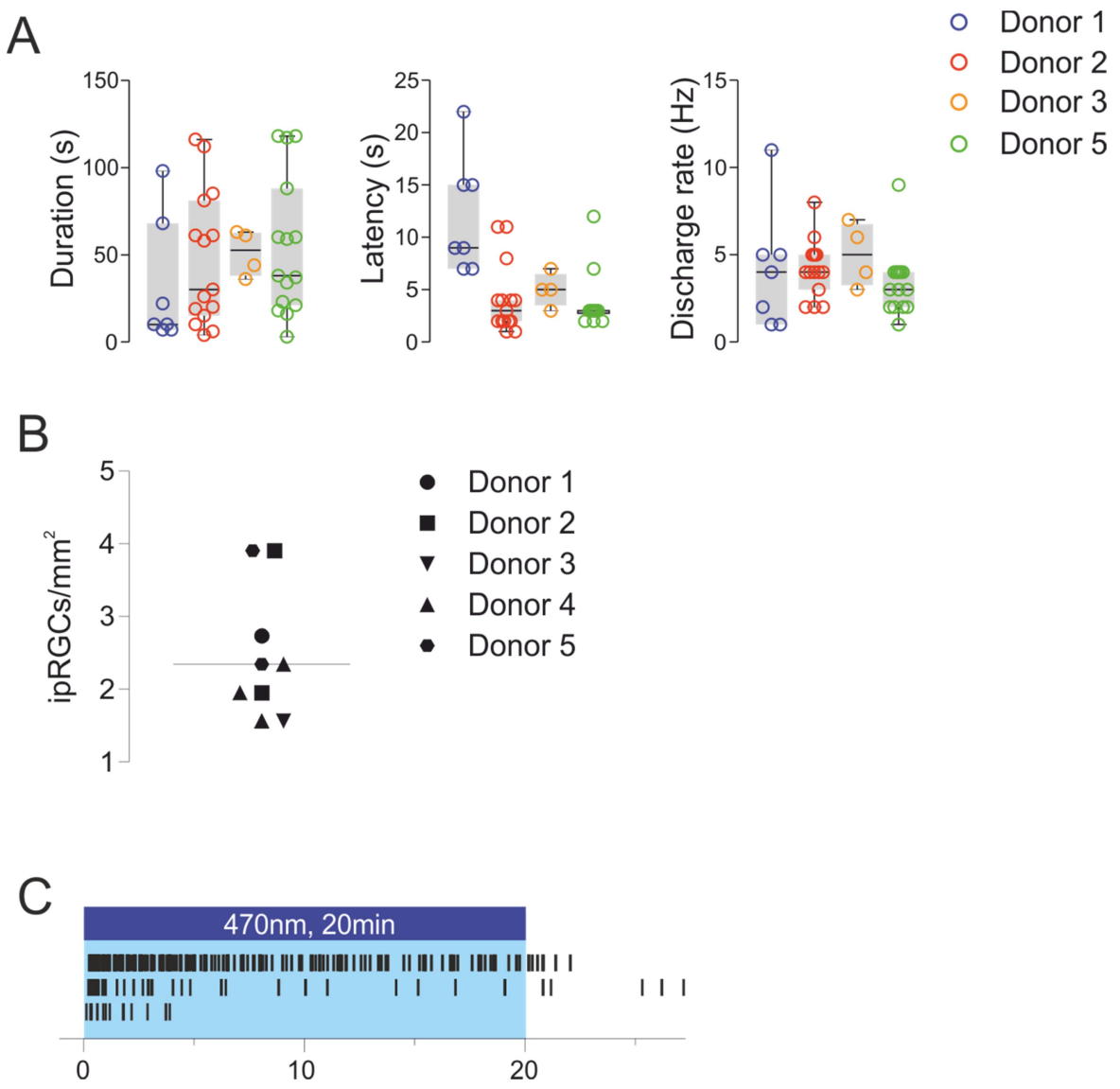

Fig. S1: A subset of human RGCs is intrinsically photosensitive. (**A**) Response average rate, peak, latency, and duration for each donors (donors 1, 2, 3, and 5, respectively n=7, 15, 4, and 15) to 30s light pulses ($2x10^{13}$ photons/cm^2/s, 470nm). (**B**) The density of responsive cells in different pieces from each donor.(**C**) Individual ipRGC responses to 20 min light stimulation (~10^{13}photons/cm^2/s, 470nm).

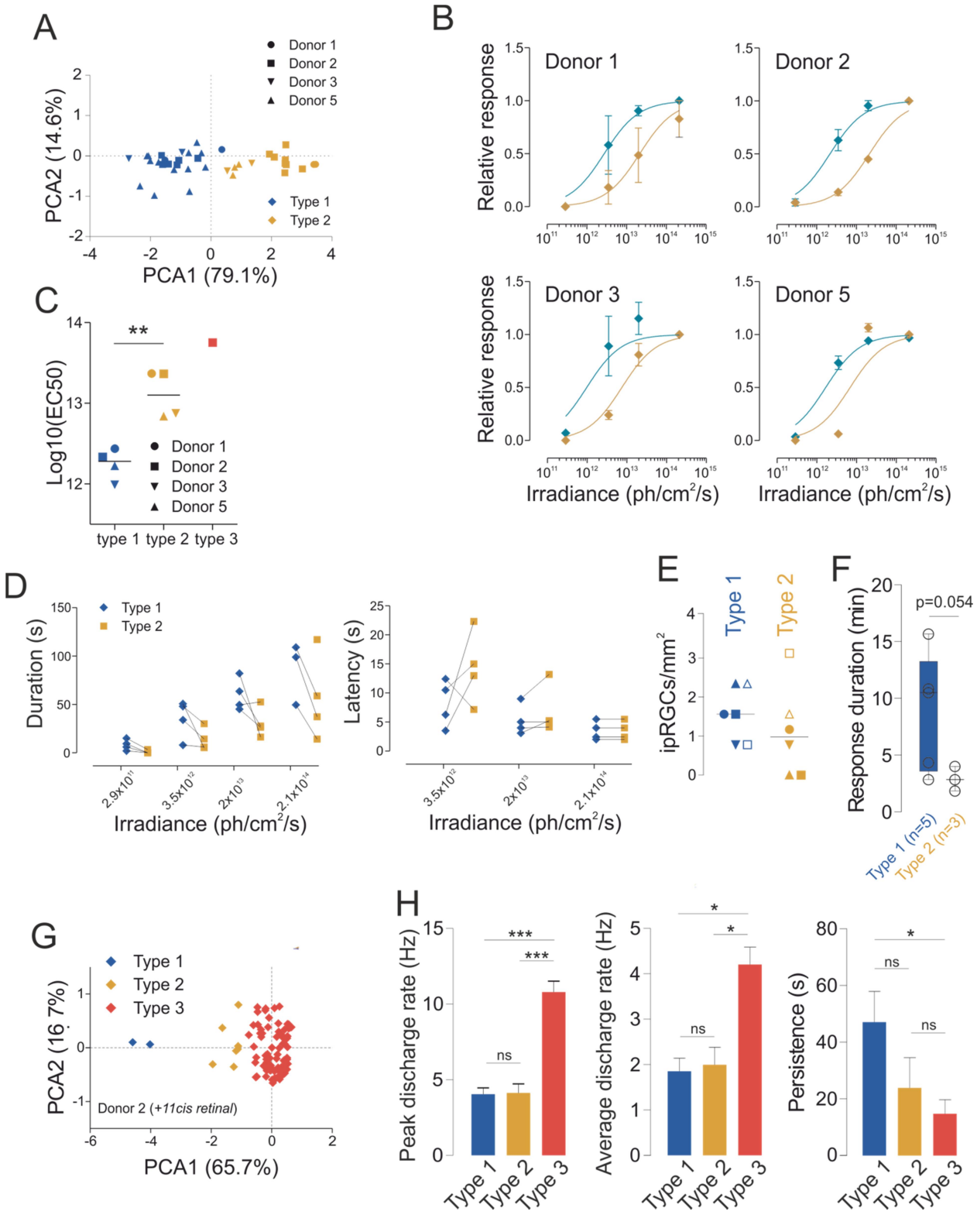
A
Donor 1
Donor 2
Donor 3
Donor 5
Type 1
Type 2
PCA2 (14.6%)
PCA1 (79.1%)
B
Donor 1
Donor 2
Donor 3
Donor 5
Relative response
Irradiance (ph/cm²/s)
C
Log10(EC50)
**
type 1 type 2 type 3
D
Duration (s)
Latency (s)
Irradiance (ph/cm²/s)
E
ipRGCs/mm²
Type 1
Type 2
F
Response duration (min)
p=0.054
Type 1 (n=5)
Type 2 (n=3)
G
Type 1
Type 2
Type 3
PCA2 (16.7%)
PCA1 (65.7%)
Donor 2 (+11cis retinal)
H
Peak discharge rate (Hz)
Average discharge rate (Hz)
Persistence (s)
ns
Type 1
Type 2
Type 3

Fig. S2: Human ipRGCs display different subtypes. (**A**) PCA of the ipRGCs response parameters (sensitivity, latency, and duration, n=42, 4 donors). (**B**) Dose-response curves by subtypes in each donor. (**C**) ipRGCs subtypes EC50 in each donor (Student t-test, p=0.00187). (**D**) ipRGCs response latency and duration in each donor by subtypes. (**E**) Density of each subtypes across donors. (**F**) Type 1 and 2 ipRGCs average response duration to 10 min light stimulations. (**G**) PCA of the ipRGCs response parameters (sensitivity, latency, and duration, n=88, 1 donor) after incubation in *11-cis* retinal. (**H**) Average ipRGCs subtypes response peak (*left*), average (*center*), and persistence (*right*) to a 30s, 470nm, $2x10^{14}$ photons/cm^2/s light stimulus (***p<0.001, *p<0.05, one-way ANOVA and Bonferroni *post hoc* tests, n=23, 19, and 78 for types 1, 2, and 3 respectively).

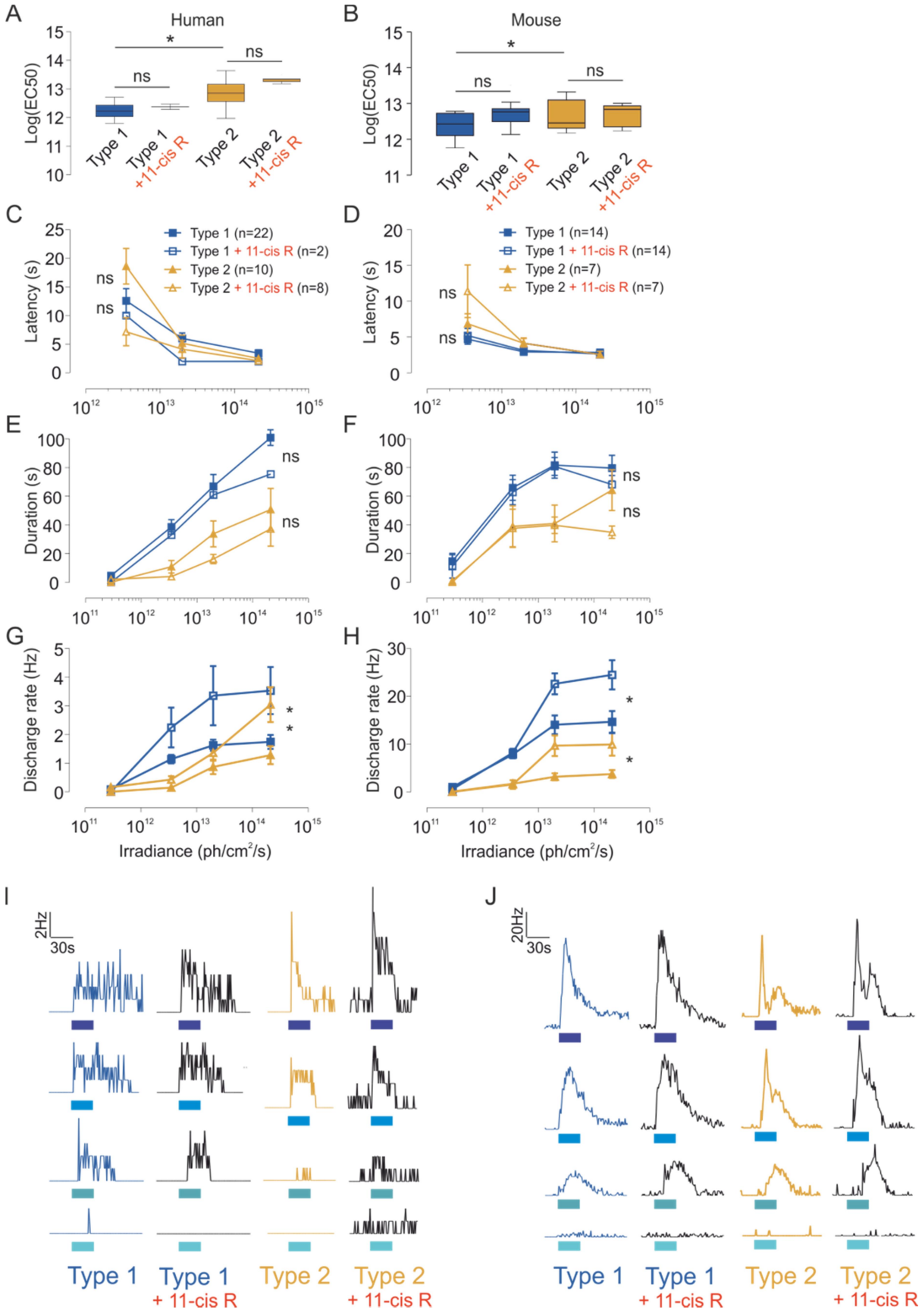
A
Human
Log(EC50)
Type 1
Type 1 +11-cis R
Type 2
Type 2 +11-cis R
ns
*
B
Mouse
C
Latency (s)
Type 1 (n=22)
Type 1 + 11-cis R (n=2)
Type 2 (n=10)
Type 2 + 11-cis R (n=8)
D
Type 1 (n=14)
Type 1 + 11-cis R (n=14)
Type 2 (n=7)
Type 2 + 11-cis R (n=7)
E
Duration (s)
F
G
Discharge rate (Hz)
Irradiance (ph/cm²/s)
H
I
2Hz
30s
Type 1
Type 1 + 11-cis R
Type 2
Type 2 + 11-cis R
J
20Hz

Fig. S3: Effect of 11-cis retinal on type 1 and 2 ipRGCs: Sensitivity, latency, duration, discharge rate, and representative time course of type 1 and 2 light responses in human (**A, C, E, G, I**) and mouse (**B, D, F, H, J**) either with or without supply of *11-cis* retinal to the medium. In humans, type 1 and 2 ipRGCs are from different donors and the same donor before/after addition of 11-cis retinal (type 1 n=22 and 2, type 2 n=10 and 8 respectively). In mice, the same type 1 and 2 cells are compared before/after addition of 11-cis retinal (type 1 n=14, type 2 n=7). (**A**) unpaired t-test, (**B**) paired t-test, and (**C-H**) 2way ANOVA. * $p<0.05$.

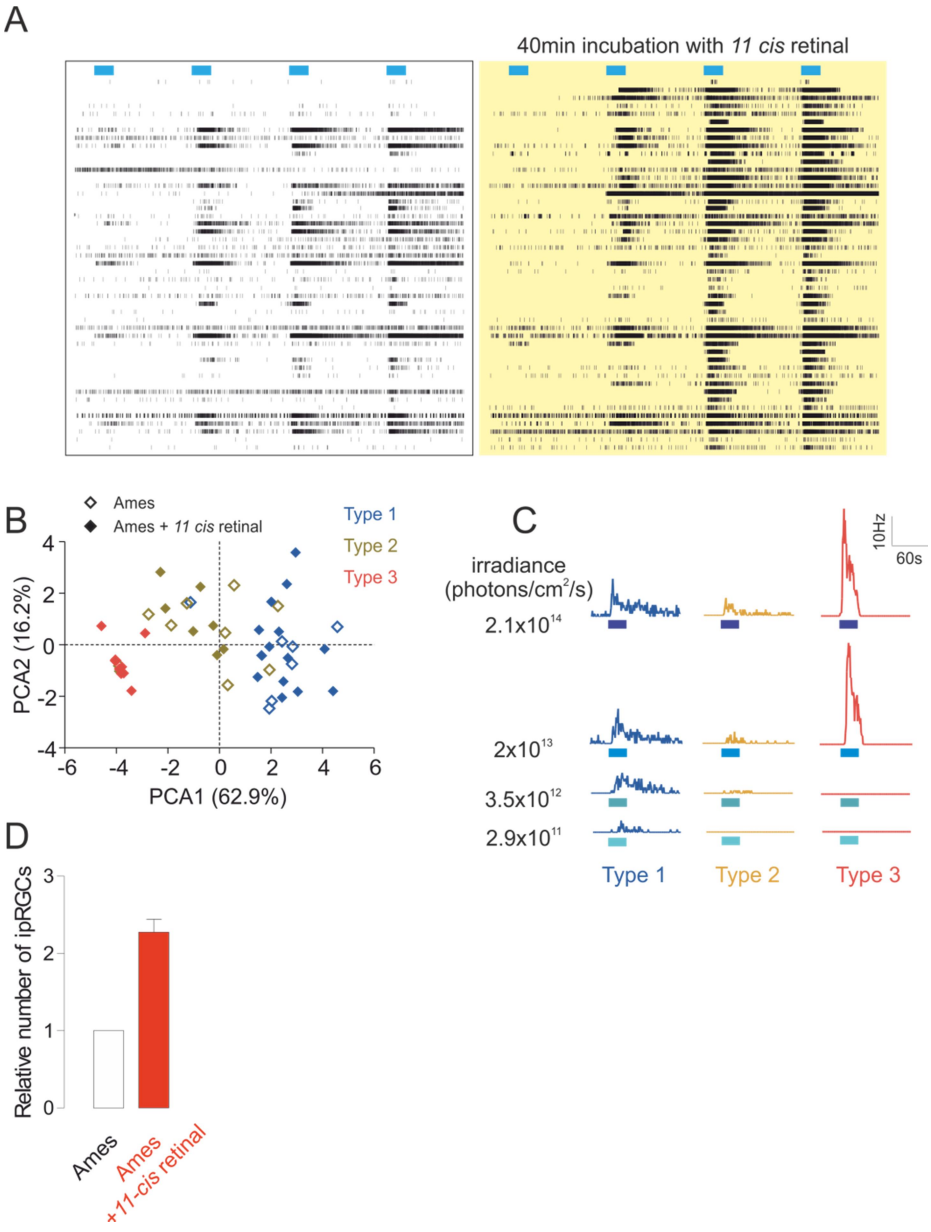

Fig. S4: Mouse ipRGCs display similar subtypes. (A) Examples of responses to light from several channels from a piece of the retina before (left panel) and after addition of *11-cis* retinal to the recording medium (*right panel*). (**B**) Corresponding PCA of ipRGCs response parameters (sensitivity, latency, and duration) before (*empty symbols*) and after (*full symbols*) addition of *11-cis* retinal to the medium. (**C**) Representative responses from type 1, 2, and 3 mouse ipRGCs to increasing irradiance light pulses (30s, from $2x10^{11}$to $2x10^{14}$ photons/cm^2/s, 470nm). *Blue bars: light pulse.* (**D**) Relative number of responding cells before and after addition of *11-cis* retinal to the medium (n= 29 and 71 cells, 3 mice).

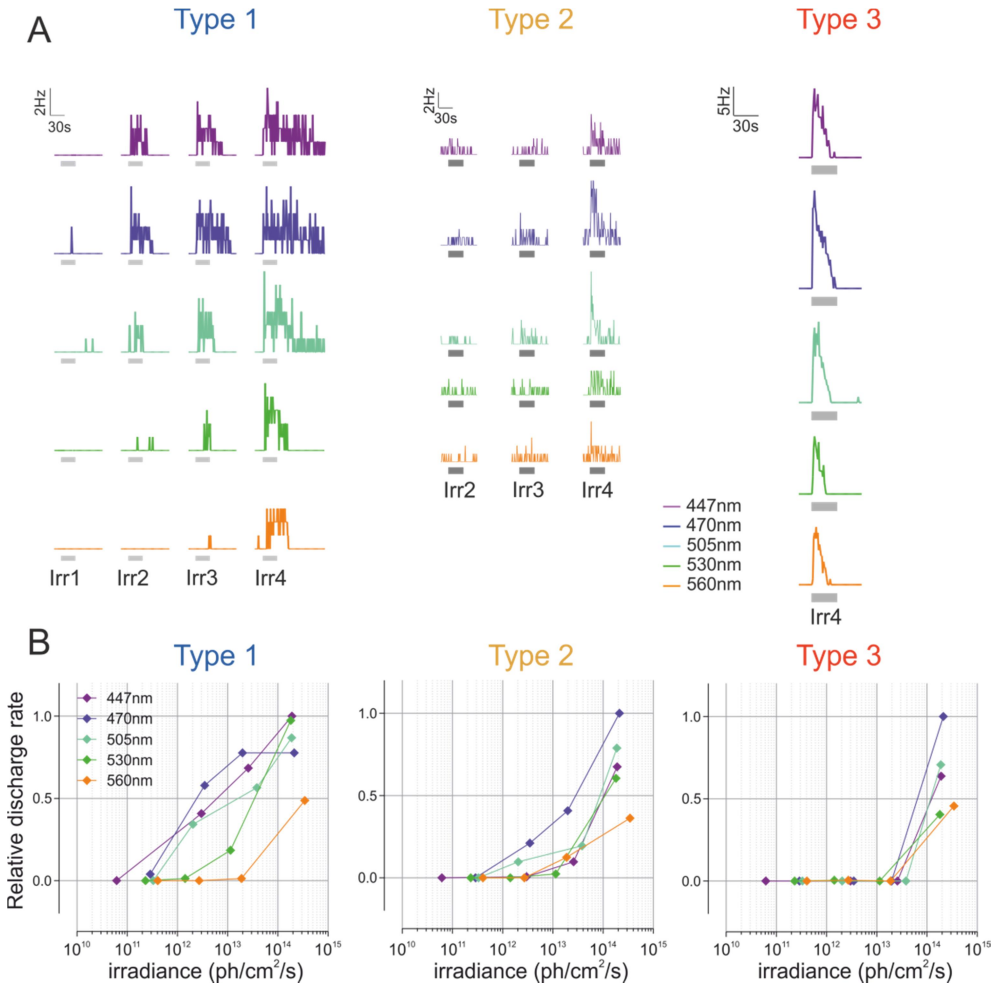

Fig. S5: Spectral functions of human ipRGCs. Traces and corresponding DRC of individual examples of type 1, 2, and 3 ipRGCs responses to 30s light pulses at different irradiances and wavelengths (Irr1 to Irr4, from $2x10^{11}$to $2x10^{14}$ photons/cm^2/s, 447, 470, 505, 530, and 560nm).

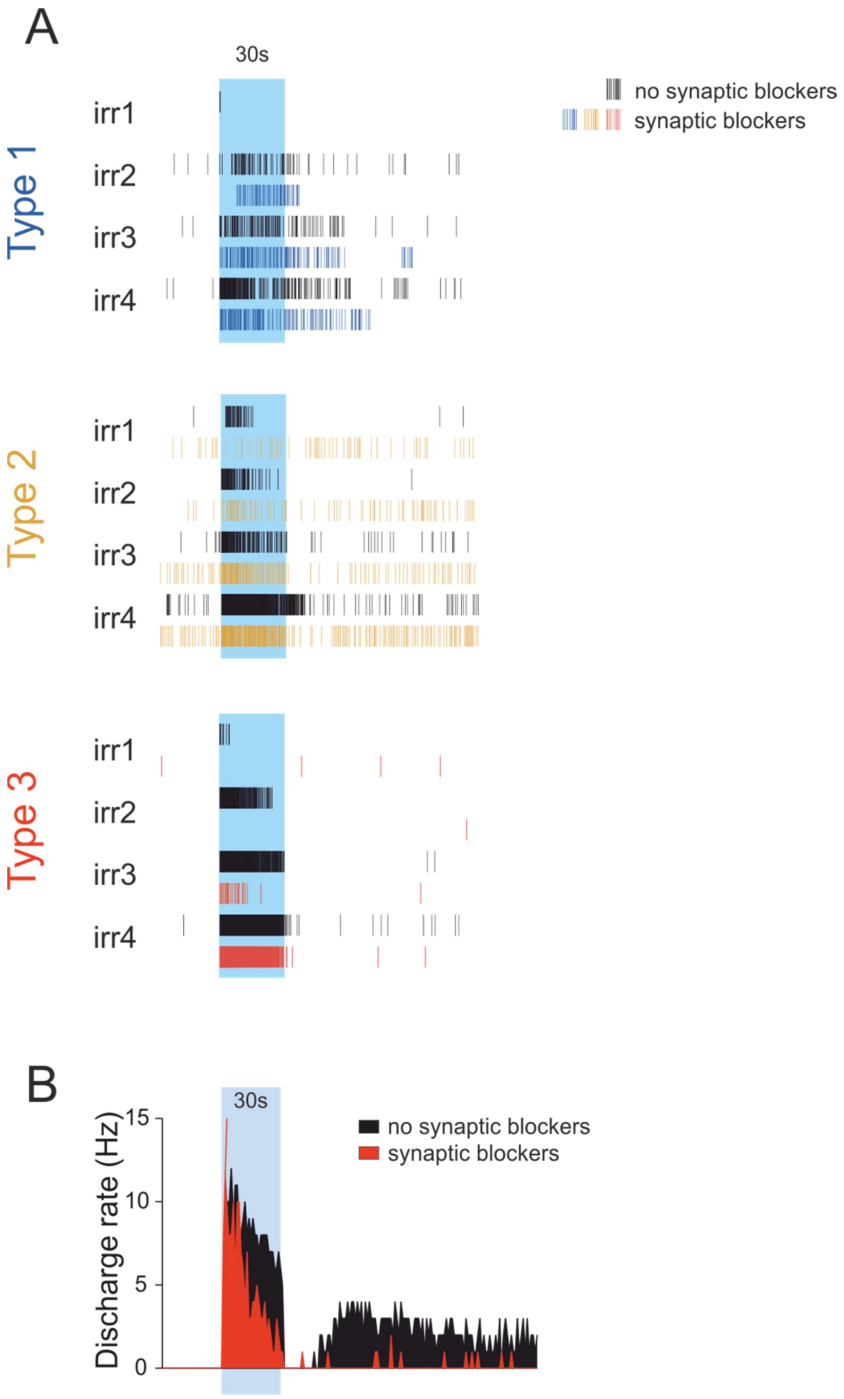

Fig. S6: Human ipRGCs integrate extrinsic signals. (**A**) Example rasters plot of type 1, 2, and 3 ipRGCs responses to increasing irradiance light pulses (30s, from $2x10^{11}$to $2x10^{14}$ photons/cm^2/s, irr1 to 4, 470nm, *blue background*) before (*black traces*) and after (*color traces*) application of synaptic blockers. (**B**) Example of extrinsic inhibited response at light OFF (30s, $2x10^{14}$ photons/cm^2/s, 470nm).

TableS1: Melanopsin-dependent visual and non-visual responses to light

	Authors	Date	Response	Stimuli	Peak (nm)	Duration (s)	Ref
Non-visual	Thapan et al.	2001	Melatonin suppression	6wl, 5-8 irr	459	1800	(*26*)
	Brainard et al.	2001	Melatonin suppression	9wl, 6-10 irr	464	5400	(*27*)
	Najjar et al.	2014	Melatonin suppression	9wl, iso irradiance	484	3600	(*28*)
	Bouma	1962	PLR	9wl, >10 irr	490	NA	(*29*)
	Gamlin et al.	2007	PLR	8wl, iso irradiance	482	10	(*30*)
	Mure et al.	2009	PLR	10wl, 6 irr	460-480	10 to 300	(*31*)
	Meylan et al.	2005	Electrical response (Heterologous expression)	5wl, iso irr	<440	10	(*32*)
	Bailes et al.	2013	Calcium increase (Heterologous expression)	6wl, 10 irr	479	2	(*33*)
	Cajochen et al.	2005	Heart rate	Blue (460nm) vs green (550nm)		7200	(*34*)
	Vandewalle et al.	2007	Working memory	Blue (470nm) vs green (550nm)		1080	(*35*)
	Vandewalle et al.	2013	Cognitive brain activity (visually blind subjects)	Blue (480nm)		2	(*36*)
Visual	Hankins and Lucas	2002	Adaptation of cone visual pathway	6wl, 5-9 irradiances	483	900	(*37*)
	Zaidi et al.	2007	Visual awareness (visually blind subjects)	9wl, iso irradiance	481	10	(*38*)
	Brown et al.	2012	Brightness discrimination	Melanopsin-targeted			(*39*)
	Spitchan et al.	2017	Visual cortex response	Melanopsin-targeted			(*40*)
	Vandewalle et al.	2018	Visual cortex response (visually blind subjects)	Blue (465nm)			(*41*)
	Allen et al.	2019	Form vision	Melanopsin-targeted			(*42*)

PLR, pupillary reflex to light; wl, wavelength; irr, irradiances

Table S2: Donors information

Donor	Sex	Age (years)	COD	TOD	Delay (hours)
1	F	74	Liver disease	2.56PM	5
2	M	54	Subarachnoid hemorrhage after trauma	2.36AM	1
3	F	48	Respiratory arrest after prescription overdose	9.25PM	0.5
4	M	55	Gastrointestinal bleed	3.36PM	1
5	F	55	Intracranial hemorrhage	8.30AM	2

Summary of the donors' information: age, sex, cause and time of death (COD and TOD) and the time between death and tissue sampling (delay).

Table S3: Human ipRGCs subtypes responses properties

	Type1 **Fast ON-slow OFF**	Type2 **Slow ON-slow OFF**	Type3 **Fast ON-Fast OFF**
Abundancy	>type2, <type3	<types 1,3	>types 1,2
Latency	short	long	short
Duration	long	long	short
Sensitivity	high	intermediate	low
11-cis retinal requirement	No	No	Yes
Extrinsic response	ON, small and transient	ON, large and sustained	ON, large and sustained, OFF
Mouse homolog	M1 (type III(*3*))	M2 (type II(*3*))	M3-6? (type I(*3*))

References and Notes

1. M. T. H. Do, K.-W. Yau, Intrinsically photosensitive retinal ganglion cells. *Physiol. Rev.* **90**, 1547–1581 (2010). doi:10.1152/physrev.00013.2010 Medline

2. T. M. Schmidt, S.-K. Chen, S. Hattar, Intrinsically photosensitive retinal ganglion cells: Many subtypes, diverse functions. *Trends Neurosci.* **34**, 572–580 (2011). doi:10.1016/j.tins.2011.07.001 Medline

3. D. C. Tu, D. Zhang, J. Demas, E. B. Slutsky, I. Provencio, T. E. Holy, R. N. Van Gelder, Physiologic diversity and development of intrinsically photosensitive retinal ganglion cells. *Neuron* **48**, 987–999 (2005). doi:10.1016/j.neuron.2005.09.031 Medline

4. X. Zhao, B. K. Stafford, A. L. Godin, W. M. King, K. Y. Wong, Photoresponse diversity among the five types of intrinsically photosensitive retinal ganglion cells. *J. Physiol.* **592**, 1619–1636 (2014). doi:10.1113/jphysiol.2013.262782 Medline

5. I. Provencio, I. R. Rodriguez, G. Jiang, W. P. Hayes, E. F. Moreira, M. D. Rollag, A novel human opsin in the inner retina. *J. Neurosci.* **20**, 600–605 (2000). doi:10.1523/JNEUROSCI.20-02-00600.2000 Medline

6. S. Nasir-Ahmad, S. C. S. Lee, P. R. Martin, U. Grünert, Melanopsin-expressing ganglion cells in human retina: Morphology, distribution, and synaptic connections. *J. Comp. Neurol.* **527**, 312–327 (2019). doi:10.1002/cne.24176 Medline

7. H.-W. Liao, X. Ren, B. B. Peterson, D. W. Marshak, K.-W. Yau, P. D. Gamlin, D. M. Dacey, Melanopsin-expressing ganglion cells on macaque and human retinas form two morphologically distinct populations. *J. Comp. Neurol.* **524**, 2845–2872 (2016). doi:10.1002/cne.23995 Medline

8. J. Hannibal, A. T. Christiansen, S. Heegaard, J. Fahrenkrug, J. F. Kiilgaard, Melanopsin expressing human retinal ganglion cells: Subtypes, distribution, and intraretinal connectivity. *J. Comp. Neurol.* **525**, 1934–1961 (2017). doi:10.1002/cne.24181 Medline

9. G. Esquiva, P. Lax, J. J. Pérez-Santonja, J. M. García-Fernández, N. Cuenca, Loss of Melanopsin-Expressing Ganglion Cell Subtypes and Dendritic Degeneration in the Aging Human Retina. *Front. Aging Neurosci.* **9**, 79 (2017). doi:10.3389/fnagi.2017.00079 Medline

10. K. A. Jones, M. Hatori, L. S. Mure, J. R. Bramley, R. Artymyshyn, S.-P. Hong, M. Marzabadi, H. Zhong, J. Sprouse, Q. Zhu, A. T. E. Hartwick, P. J. Sollars, G. E. Pickard, S. Panda, Small-molecule antagonists of melanopsin-mediated phototransduction. *Nat. Chem. Biol.* **9**, 630–635 (2013). doi:10.1038/nchembio.1333 Medline

11. K. Y. Wong, A retinal ganglion cell that can signal irradiance continuously for 10 hours. *J. Neurosci.* **32**, 11478–11485 (2012). doi:10.1523/JNEUROSCI.1423-12.2012 Medline

12. K. Y. Wong, F. A. Dunn, D. M. Graham, D. M. Berson, Synaptic influences on rat ganglion-cell photoreceptors. *J. Physiol.* **582**, 279–296 (2007). doi:10.1113/jphysiol.2007.133751 Medline

13. D. M. Berson, F. A. Dunn, M. Takao, Phototransduction by retinal ganglion cells that set the circadian clock. *Science* **295**, 1070–1073 (2002). doi:10.1126/science.1067262 Medline

14. D. Karnas, D. Hicks, J. Mordel, P. Pévet, H. Meissl, Intrinsic photosensitive retinal ganglion cells in the diurnal rodent, Arvicanthis ansorgei. *PLOS ONE* **8**, e73343 (2013). doi:10.1371/journal.pone.0073343 Medline

15. D. M. Dacey, H.-W. Liao, B. B. Peterson, F. R. Robinson, V. C. Smith, J. Pokorny, K.-W. Yau, P. D. Gamlin, Melanopsin-expressing ganglion cells in primate retina signal colour and irradiance and project to the LGN. *Nature* **433**, 749–754 (2005). doi:10.1038/nature03387 Medline

16. L. E. Quattrochi, M. E. Stabio, I. Kim, M. C. Ilardi, P. Michelle Fogerson, M. L. Leyrer, D. M. Berson, The M6 cell: A small-field bistratified photosensitive retinal ganglion cell. *J. Comp. Neurol.* **527**, 297–311 (2019). doi:10.1002/cne.24556 Medline

17. Y. Fu, H. Zhong, M.-H. H. Wang, D.-G. Luo, H.-W. Liao, H. Maeda, S. Hattar, L. J. Frishman, K.-W. Yau, Intrinsically photosensitive retinal ganglion cells detect light with a vitamin A-based photopigment, melanopsin. *Proc. Natl. Acad. Sci. U.S.A.* **102**, 10339–10344 (2005). doi:10.1073/pnas.0501866102 Medline

18. S. Panda, I. Provencio, D. C. Tu, S. S. Pires, M. D. Rollag, A. M. Castrucci, M. T. Pletcher, T. K. Sato, T. Wiltshire, M. Andahazy, S. A. Kay, R. N. Van Gelder, J. B. Hogenesch, Melanopsin is required for non-image-forming photic responses in blind mice. *Science* **301**, 525–527 (2003). doi:10.1126/science.1086179 Medline

19. T. D. Lamb, Photoreceptor spectral sensitivities: Common shape in the long-wavelength region. *Vision Res.* **35**, 3083–3091 (1995). doi:10.1016/0042-6989(95)00114-F Medline

20. G. W. Weinstein, R. R. Hobson, F. H. Baker, Extracellular recordings from human retinal ganglion cells. *Science* **171**, 1021–1022 (1971). doi:10.1126/science.171.3975.1021 Medline

21. T. W. Kraft, D. M. Schneeweis, J. L. Schnapf, Visual transduction in human rod photoreceptors. *J. Physiol.* **464**, 747–765 (1993). doi:10.1113/jphysiol.1993.sp019661 Medline

22. Z. Jiang, W. W. S. Yue, L. Chen, Y. Sheng, K.-W. Yau, Cyclic-Nucleotide- and HCN-Channel-Mediated Phototransduction in Intrinsically Photosensitive Retinal Ganglion Cells. *Cell* **175**, 652–664.e12 (2018). doi:10.1016/j.cell.2018.08.055 Medline

23. N. L. Mata, R. A. Radu, R. S. Clemmons, G. H. Travis, Isomerization and oxidation of vitamin a in cone-dominant retinas: A novel pathway for visual-pigment regeneration in daylight. *Neuron* **36**, 69–80 (2002). doi:10.1016/S0896-6273(02)00912-1 Medline

24. C. D. Bridges, R. A. Alvarez, S. L. Fong, Vitamin A in human eyes: Amount, distribution, and composition. *Invest. Ophthalmol. Vis. Sci.* **22**, 706–714 (1982). Medline

25. M. T. Flood, C. D. Bridges, R. A. Alvarez, W. S. Blaner, P. Gouras, Vitamin A utilization in human retinal pigment epithelial cells in vitro. *Invest. Ophthalmol. Vis. Sci.* **24**, 1227–1235 (1983). Medline

26. K. Thapan, J. Arendt, D. J. Skene, An action spectrum for melatonin suppression: Evidence for a novel non-rod, non-cone photoreceptor system in humans. *J. Physiol.* **535**, 261–267 (2001). doi:10.1111/j.1469-7793.2001.t01-1-00261.x Medline

27. G. C. Brainard, J. P. Hanifin, J. M. Greeson, B. Byrne, G. Glickman, E. Gerner, M. D. Rollag, Action spectrum for melatonin regulation in humans: Evidence for a novel circadian photoreceptor. *J. Neurosci.* **21**, 6405–6412 (2001). doi:10.1523/JNEUROSCI.21-16-06405.2001 Medline

28. R. P. Najjar, C. Chiquet, P. Teikari, P.-L. Cornut, B. Claustrat, P. Denis, H. M. Cooper, C. Gronfier, Aging of non-visual spectral sensitivity to light in humans: Compensatory mechanisms? *PLOS ONE* **9**, e85837 (2014). doi:10.1371/journal.pone.0085837 Medline

29. H. Bouma, Size of the static pupil as a function of wavelength and luminosity of the light incident on the human eye. *Nature* **193**, 690–691 (1962). doi:10.1038/193690a0 Medline

30. P. D. R. Gamlin, D. H. McDougal, J. Pokorny, V. C. Smith, K.-W. Yau, D. M. Dacey, Human and macaque pupil responses driven by melanopsin-containing retinal ganglion cells. *Vision Res.* **47**, 946–954 (2007). doi:10.1016/j.visres.2006.12.015 Medline

31. L. S. Mure, P.-L. Cornut, C. Rieux, E. Drouyer, P. Denis, C. Gronfier, H. M. Cooper, Melanopsin bistability: A fly's eye technology in the human retina. *PLOS ONE* **4**, e5991 (2009). doi:10.1371/journal.pone.0005991 Medline

32. Z. Melyan, E. E. Tarttelin, J. Bellingham, R. J. Lucas, M. W. Hankins, Addition of human melanopsin renders mammalian cells photoresponsive. *Nature* **433**, 741–745 (2005). doi:10.1038/nature03344 Medline

33. H. J. Bailes, R. J. Lucas, Human melanopsin forms a pigment maximally sensitive to blue light (λmax $\approx$ 479 nm) supporting activation of G(q/11) and G(i/o) signalling cascades. *Proc. Biol. Sci.* **280**, 20122987 (2013). doi:10.1098/rspb.2012.2987 Medline

34. C. Cajochen, M. Münch, S. Kobialka, K. Kräuchi, R. Steiner, P. Oelhafen, S. Orgül, A. Wirz-Justice, High sensitivity of human melatonin, alertness, thermoregulation, and heart rate to short wavelength light. *J. Clin. Endocrinol. Metab.* **90**, 1311–1316 (2005). doi:10.1210/jc.2004-0957 Medline

35. G. Vandewalle, S. Gais, M. Schabus, E. Balteau, J. Carrier, A. Darsaud, V. Sterpenich, G. Albouy, D. J. Dijk, P. Maquet, Wavelength-dependent modulation of brain responses to a working memory task by daytime light exposure. *Cereb. Cortex* **17**, 2788–2795 (2007). doi:10.1093/cercor/bhm007 Medline

36. G. Vandewalle, O. Collignon, J. T. Hull, V. Daneault, G. Albouy, F. Lepore, C. Phillips, J. Doyon, C. A. Czeisler, M. Dumont, S. W. Lockley, J. Carrier, Blue light stimulates cognitive brain activity in visually blind individuals. *J. Cogn. Neurosci.* **25**, 2072–2085 (2013). doi:10.1162/jocn_a_00450 Medline

37. M. W. Hankins, R. J. Lucas, The primary visual pathway in humans is regulated according to long-term light exposure through the action of a nonclassical photopigment. *Curr. Biol.* **12**, 191–198 (2002). doi:10.1016/S0960-9822(02)00659-0 Medline

38. F. H. Zaidi, J. T. Hull, S. N. Peirson, K. Wulff, D. Aeschbach, J. J. Gooley, G. C. Brainard, K. Gregory-Evans, J. F. Rizzo 3rd, C. A. Czeisler, R. G. Foster, M. J. Moseley, S. W. Lockley, Short-wavelength light sensitivity of circadian, pupillary, and visual awareness in humans lacking an outer retina. *Curr. Biol.* **17**, 2122–2128 (2007). doi:10.1016/j.cub.2007.11.034 Medline

39. T. M. Brown, S. Tsujimura, A. E. Allen, J. Wynne, R. Bedford, G. Vickery, A. Vugler, R. J. Lucas, Melanopsin-based brightness discrimination in mice and humans. *Curr. Biol.* **22**, 1134–1141 (2012). doi:10.1016/j.cub.2012.04.039 Medline

40. M. Spitschan, A. S. Bock, J. Ryan, G. Frazzetta, D. H. Brainard, G. K. Aguirre, The human visual cortex response to melanopsin-directed stimulation is accompanied by a distinct perceptual experience. *Proc. Natl. Acad. Sci. U.S.A.* **114**, 12291–12296 (2017). doi:10.1073/pnas.1711522114 Medline

41. G. Vandewalle, M. J. van Ackeren, V. Daneault, J. T. Hull, G. Albouy, F. Lepore, J. Doyon, C. A. Czeisler, M. Dumont, J. Carrier, S. W. Lockley, O. Collignon, Light modulates oscillatory alpha activity in the occipital cortex of totally visually blind individuals with intact non-image-forming photoreception. *Sci. Rep.* **8**, 16968 (2018). doi:10.1038/s41598-018-35400-9 Medline

42. A. E. Allen, F. P. Martial, R. J. Lucas, Form vision from melanopsin in humans. *Nat. Commun.* **10**, 2274 (2019). doi:10.1038/s41467-019-10113-3 Medline